Antimicrobial activity of some celastroloids and their derivatives

Marielle Cascaes Inácio[1]· Tiago Antunes Paz[2]· E. M. Kithsiri Wijeratne[1]· G. M. Kamal B. Gunaherath[1]· Rafael V. C. Guido[3]· A. A. Leslie Gunatilaka[1]

✉ A. A. Leslie Gunatilaka
leslieg1@email.arizona.edu

[1]Southwest Center for Natural Products Research, School of Natural Resources and the Environment, College of Agriculture and Life Sciences, University of Arizona, 250 E. Valencia Road, Tucson, Arizona 85706, USA

[2]Institute of Chemistry, São Paulo State University - UNESP, Rua Prof. Francisco Degni, 55, Quitandinha, Araraquara, SP 14800-060, Brazil

[3]São Carlos Institute of Physics, University of São Paulo, Av. Joao Dagnone, 1100 Jardim Santa Angelina, São Carlos, SP, 13563-120, Brazil

Abstract

Infections are among the 10 deadliest diseases in the world. Here we screened 19 celastroloids and their derivatives **1**–**19** against several strains of bacteria and yeast of biomedical significance. In general, quinonemethide-type celastroloids, except isoiguesterin (**8**) exhibited significant antibacterial activity for *Staphylococcus aureus* ATCC 25923, MRSA ATCC 33592, and the clinical isolate STA6 with MICs of 0.39–12.50 µg/mL, whereas 14(15)-enequinonemethide, balaenol (**12**), showed antifungal activity against *Candida albicans* ATCC 10261 with an MIC of 3.12 µg/mL. Among the phenolic triterpenes and their derivatives, zeylasterone (**14**) had an MIC of 1.56 µg/mL for all 3 strains of *S. aureus*, and zeylasteral (**15**) was active against *C. albicans* at 3.12 µg/mL. Cytotoxicity assays revealed that most quinonemethides were cytotoxic with IC_{50}s of 0.16–0.36 µg/mL that are below their MIC values. However, 14(15)-enequinonemethide **12** and phenolic triterpenes **14** and **15** exhibited antimicrobial activity at sub-cytotoxic concentrations, suggesting that these celastroloids are potential candidates for further studies. Molecular docking studies were used to investigate the theoretical affinities for potential protein targets of **12** and **14** in *S. aureus*, and **15** in *C. albicans*. Based on their docking scores, it can be inferred that **12** and **14** inhibits GyrB in *S. aureus*, and **15** inhibits Bdf1 in *C. albicans*.

Graphical abstract

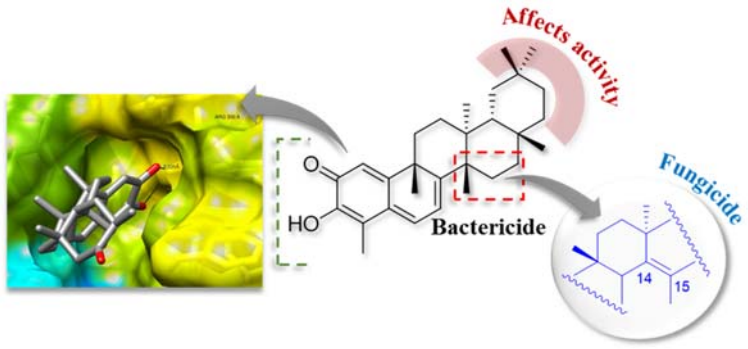

Keywords celastroloids; quinonemethide triterpenes; enequinonemethide triterpenes; phenolic triterpenes; antimicrobial activity

Introduction

Infections are among the ten deadliest diseases in the world [1]. Among other reasons, this is mainly due to the microbial resistance acquired to the conventional antibiotics which could occur through the activation of efflux pumps, destruction and modification of compounds through enzymes or mutations on the microbial proteins that results in loss of affinity by the antibiotic [2]. Natural products (NPs) and their derivatives are promising sources of new antimicrobials with various mechanisms of action [3]. In addition, co-occurrence of NPs with the same structural scaffold enable structure-activity relationship (SAR) studies that are important for the development of improved inhibitors as drug candidates [4]. Among antimicrobial NPs, triterpenes constitute a potential source due to their structural diversity [5–8].

In our search for NP-based antimicrobials, we screened a small library of natural celastroloids (quinonemethide and phenolic triterpenoids) obtained from plants of the Celastraceae family and some of their derivatives [9–13] against Gram-negative and Gram-positive bacteria and yeasts. Plants of this family have attracted attention because they contain bioactive celastroloids [14–16] and their use in Asian and South American traditional medicines in different formulations as antimicrobial (antibacterial, antifungal, and antiviral) agents [14]. For example, *Tripterygium wilfordii* is widely used in traditional Chinese medicine for the treatment of leprosy (*Mycobacterium leprae*) [14] while *Maytenus ilicifolia* is used in South American folk medicine to treat tuberculosis (usually caused by *Mycobacterium tuberculosis*) [15].

Herein we report the antibacterial and antifungal activities of sixteen celastroloids (**1–15** and **17**) and three derivatives (**16**, **18**, and **19**) against three strains of *S. aureus* (ATCC 25923, MRSA ATCC 33592, and a clinical isolate STA6) and a strain of *C. albicans* (ATCC 10261) by assessing the minimum inhibitory concentration (MIC) and minimum bactericidal/fungicidal concentration (MBC/MFC). To analyze the antimicrobial activity and determine the structure-activity relationships (SARs) of the celastroloids tested, we separated celastroloids into three groups based on their structural features as quinonemethides, 14(15)-enequinonemethides, and derivatives of pristimerin which included the phenolic triterpenoids (Figure 1). Cytotoxic activities of celastroloids exhibiting

antimicrobial activity were also tested against the normal human foreskin fibroblast cells, WI-38. Molecular docking studies were carried out with selected celastroloids with antimicrobial activity to interpret the data obtained and investigate the theoretical affinity for potential molecular targets.

Results and discussion

The celastroloids **1–15** and **17** and their derivatives **16**, **18** and **19** (Figure 1) were evaluated for their antimicrobial activity against the bacterial strains, *Escherichia coli* ATCC 25922, *Pseudomonas aeruginosa* ATCC 10197, *Staphylococcus aureus* ATCC 25923, *S. aureus* MRSA ATCC 33592, *S. aureus* STA6 (clinical isolate), and the fungus *Candida albicans* ATCC 10261. Many of the compounds tested were active against different strains of *S. aureus* and *C. albicans* (see Tables 1–3). To understand SARs, the data obtained are categorized under three groups: (A) quinonemethide triterpenes (QMTs) with different substituents in ring E (Figure 1, Group A); (B) QMTs with C-14(15) double bond associated with 14→15 methyl shift (enequinonemethides) containing different substituents in ring E (Figure 1, Group B); and (C) pristimerin derivatives with the same E-ring and differences in rings A, B, and C (Figure 1, Group C). For the purpose of comparison, that data for pristimerin (**4**) was included in Tables 1 and 3.

The results showed that all compounds tested except the 6-oxophenolic celastroloid, zeylasterone (**14**), had no activity against the Gram-negative bacteria (*E. coli*, and *P. aeruginosa*) which is in agreement with the literature data [17–24]. However, **14** exhibited poor inhibitory activity against *P. aeruginosa* ATCC 10197, with an MIC value of 25 μg/mL and an MBC value of 50 μg/mL (Supplementary data, Table S1).

Antibacterial activity against *S. aureus*

It is apparent that different functional groups present in ring E of QMTs have an impact on the antimicrobial activity against *S. aureus* ATCC 25923. The most potent compounds were tingenone (**1**), 30-hydroxypristimerin (**5**) and 22β-hydroxytingenone (**6**), each showing an MIC value of 0.39 μg/mL (Table 1). Tingenone (maytenin, **1**) has a carbonyl group at C-21, while **6** has a β-OH group at C-22 in addition to the C-21 carbonyl function, and **5** lacks both these groups, but has an α-

CO_2Me group and a β-CH_2OH at C-20. Tingenol (maytenol, **2**), celastrol (**3**) and 20α-hydroxytingenone (**7**) exhibited decreased inhibitory activity compared to **1**, **5**, and **6**, each showing an MIC value of 0.78 μg/mL (Table 1). Tingenol (**2**) is the C-21 reduced product of compound **1**. Celastrol (**3**) has an α-CO_2H group at C-20 whereas pristimerin (**4**) has an α-CO_2Me at C-20. Compound **7** differs from **6** by the position of the hydroxy substituent in ring E. Isoiguesterin (**8**) was less potent than its 29-hydroxy-20(29)-dihydro analogue, isoiguesterinol (**9**). The lowest MBC value was observed for 30-hydroxypristimerin (**5**) (0.78 μg/mL), followed by tingenone (**1**) (1.56 μg/mL). All the compounds in Group A showed bactericidal effect except for isoiguesterin (**8**). Compounds **1–3**, **5–7** and **9** showed antibacterial activity with MIC values below 10 μg/mL, which is considered to be significant [5,25]. Even though most of the QMTs showed antimicrobial activity for all *S. aureus* strains tested, the susceptibility for each strain was different (Table 1). Methicillin-resistant *S. aureus* (MRSA) was susceptible to a number of QMTs. Thus, compounds **1–3**, **5–7**, and **9** showed MIC and MBC values of < 10 μg/mL. All QMTs showed antibacterial effect against MRSA. The clinical isolate of *S. aureus* STA6 was less susceptible to the QMTs, except for **1** and **6** which had MBC values of < 10 μg/mL.

The MIC values for the 14(15)-enequinonemethide triterpenes [14(15)-eneQMTs], balaenonol (**10**), balaenol (**12**), and isobalaenol (**13**), also found in plants of the family Celastraceae [16], against *S. aureus* ATCC 25923 were determined to be 1.56 μg/mL while for isobalaendiol (**11**) it was 6.25 μg/mL (Table 2). Considering the MBC value, balaenonol (**10**) was the most potent against this strain among the 14(15)-eneQMTs (Group B). However, it was less potent than **1** and **5** (QMTs, Group A). Balaenol (**12**) was the most potent compound against MRSA ATCC 33592 (MIC = 0.19 μg/mL), while the MIC of balaenonol (**10**) against the same bacterial strain was found to be 1.56 μg/mL. Both **10** and **12** showed considerable inhibitory activity (MIC and MBC < 10 μg/mL) against this strain. *S. aureus* STA6 strain was less susceptible to this group of compounds with only **10** having an MBC value < 10 μg/mL (Table 2). It was observed that the MIC and MBC values of **12** against *S. aureus* ATCC 25923 were two-fold lower than that of **2**. However, **12** showed four-fold higher inhibitory activity compared to **2** against the MRSA strain. Balaenol (**12**) showed two-fold

higher inhibitory activity against the clinical strain STA6 compared to **2**, but both showed the same MBC value (25 μg/mL).

In group C, all the compounds tested have the same E ring, but different substituents in rings A–C. Zeylasterone (**14**) was the most potent compound against all *S. aureus* strains (Table 3). This compound has two hydroxy substituents at C-2 and C-3, and a CO_2H group at C-4 all of which are in ring A, and a carbonyl group at C-6 (ring B). The SAR investigation indicated that the CO_2H group at C-4 of **14** favorably contributed to its antimicrobial activity. This finding is supported by the fact that **14** showed considerably improved potency compared to **15** (in which the 4-CO_2H group has been replaced by a CHO group) against *S. aureus* ATCC 25923 (> 30-fold), MRSA (ca. 16-fold), and STA6 (ca. 8-fold). In contrast, the presence of methoxy substituents at C-2 and C-3 in ring A (derivatives **16** and **18**) or acetyl substituents at C-2 and C-3 (**19**) were detrimental to the antibacterial activity. Pristimerinene (**17**) with a 9(11)-double bond in ring C and the methyl group at C-9 shifted to C-11 showed poor antibacterial activity in comparison to pristimerin (**4**). These results suggest that, although the quinonemethide skeleton is as important for antimicrobial activity as the substituents in ring E, some substituents in rings A and B could potentiate the antibacterial activity of this series of celastroloids.

Antifungal activity against *C. albicans*

It was also observed that the presence of some functional groups in ring E is essential for the antifungal activity against *C. albicans*. However, the most potent compounds were different from those identified to be active against *S. aureus*, except for the QMT, 30-hydroxypristimerin (**5**). The most potent QMTs were celastrol (**3**) and **5** (MIC value = 6.25 μg/mL, Table 1). Compound **5** has methoxycarbonyl (CO_2Me) and hydroxymethylene (CH_2OH) substituents at C-20, while **3** has only a CO_2H substituent at this position. The most potent compounds against *S. aureus* ATCC 25923, tingenone (**1**) and 22β-hydroxytingenone (**6**) showed decreased inhibitory activity against *C. albicans* (MIC = 50 μg/mL). The same MIC value was observed for 20α-hydroxytingenone (**7**) against *C. albicans*. Isoiguesterin (**8**) and isoiguesterinol (**9**) were poor *C. albicans* inhibitors (MIC

>100 μg/mL). The lowest MFC value was observed for 30-hydroxypristimerin (**5**) (50 μg/mL) followed by celastrol (**3**) (100 μg/mL). The other QMTs did not show any antifungal activity.

All 14(15)-enequinonemethides exhibited some antifungal activity (Table 2). Balaenol (**12**) showed the lowest MIC value (3.12 μg/mL) and its C-20 epimer, isobalaenol (**13**) showed the lowest MFC value (6.25 μg/mL). Thus, these two compounds (**12** and **13**) were more potent than the QMTs (Group A). Comparing the QMT **2** with its 14(15)-ene-QMT **12**, it was observed that the inhibitory activity of **12** was ca. 16-fold greater for *C. albicans*. These results differ from those obtained for *S. aureus* suggesting that the molecular mechanisms of action of these celastroloids may be different in these microorganisms.

For the celastroloids of Group C (Figure 1, Table 3), antifungal activities against *C. albicans* were found to be different from antibacterial activities against *S. aureus*. Zeylasteral (**15**) (MIC value = 3.12 μg/mL), containing an aldehyde group at C-4, was 2-fold more potent than the corresponding carboxylic acid analog, zeylasterone (**14**) (6.25 μg/mL). The methoxylated and acetylated derivatives (**16**, **18**, and **19**), as well as pristimerinene (**17**) having the 9(11)-double bond associated with 9→11 methyl shift were not active against *C. albicans*, demonstrating the importance of the rings A, B, and C in exhibiting antifungal activity. The greatest antifungal activity in this group was observed for zeylasteral (**15**) with an MFC value of 3.12 μg/mL.

Cytotoxicity evaluation

Celastroloids (mainly QMTs) are also known for their cytotoxic effects which restrict their clinical applications [26]. However, due their high pharmaceutical potential, structural modifications have been made to obtain less toxic analogues/derivatives [27]. Here, we evaluated the cytotoxicity (IC_{50}) of the most potent compounds as representatives of each series using the normal human foreskin fibroblast (WI-38) cells (Table 4, Table S3). Most QMTs showed cytotoxic activity at concentrations lower than their MIC values. However, balaenol (**12**) showed activity against MRSA (MIC = 0.19 μg/mL) at a sub-cytotoxic concentration (IC_{50} = 1.27 μg/mL) suggesting that it may be a candidate for further development as an antibacterial agent. *C. albicans* was sensitive to zeylasteral (**15**, MIC =

3.12 μg/mL) at a lower concentration than that observed in the cytotoxic assay (IC_{50} = 6.38 μg/mL). Similarly, zeylasterone (**14**) showed inhibitory activity (MIC = 1.56 μg/mL) against all *S. aureus* strains tested at a sub-cytotoxic concentration (IC_{50} = 2.85 μg/mL) suggesting these celastroloids are potential candidates for further medicinal chemistry studies.

Docking Studies

Previous studies have shown that celastroloids have multiple targets in microorganisms including interaction with the lipid layer, permeability changing of the cytoplasmic membrane, cell wall synthesis inhibition, and respiration impairment of intact cells [7,17,20,28,29]. Docking studies were performed to predict the binding affinity between the most potent celastroloids (< 10 μg/mL) and potential target proteins from *S. aureus*, including DNA gyrase B (GyrB - DNA replication), dihydrofolate reductase (DHFR), and penicillin binding protein 2a (PBP2a). The same strategy was applied to determine putative targets of *C. albicans* including the secreted aspartic proteinase (candidapepsin 2), bromodomain-containing factor 1 (Bdf1), and glyculpeptide N-tetradecanoyltransferase (N- myristoyltransferase - Nmt). These are relevant and attractive targets for antimicrobial drug discovery (see below). Thus, balaenol (**12**) and zeylasterone (**14**) were modeled within the binding pockets of these targets from *S. aureus*, whereas zeylasteral (**15**) was modeled in the putative targets from *C. albicans* since they had antimicrobial activities at sub-cytotoxic concentrations and showed reasonable selectivity to bacterial and fungal cells, respectively (Table 4, Table S3). The estimation of the binding energy was evaluated by the AutoDock Vina scoring function (Supplementary data, Table S4-S9) [30]. In general, we observed that the active compounds had low score values and interacted with key residues in the proteins pocket. These findings indicate that the ligand-receptor interaction occurs in different proteins (Supplementary data, Table S4–S9, Figure S1).

DNA gyrases (Gyr) are highly conserved type II topoisomerases acting in the DNA replication and transcription. GyrB is an interesting antibacterial drug target for *S. aureus* including MRSA [31,32]. GyrB (PDB ID, 3TTZ) used in the docking studies has been crystallized with the

inhibitor 3-fluorosubstituted piperidine (pyrrolamides) [33]. The celastroloids, balaenol (**12**) and zeylasterone (**14**) showed five hydrophobic interactions each with key residues from the active site of GyrB (Figure 2A–C, Table S4). Zeylasterone (**14**) also showed a favorable hydrogen bond with the Asn54 residue.

Dihydrofolate reductase (DHFR) reduces dihydrofolate (DHF) to tetrahydrofolate (THF). This enzyme plays a central role in the biosynthesis of folic acid in bacteria [34,35]. DHFR (PDB ID, 3FYW) used in the docking studies has been crystallized with the inhibitor iclaprim [36]. Balaenol (**12**) showed six hydrophobic interactions and two hydrogens bonds with the key residues within DHFR binding site, including Val31 and Phe92 residues (Figure 2D and 2F, Table S5). Zeylasterone (**14**) showed eight hydrophobic interactions and one hydrogen bond to the binding site residues. In this case, key interactions were predicted with Ile50 and Phe92 residues (Figure 2E and 2F, Table S5).

Penicillin binding protein 2a (PBP2a) is essential for the peptidoglycan biosynthesis that constitutes the bacteria cell wall [37]. PBPs are the target for β-lactam antibiotics and PBP2a is regarded as the main target underlying the MRSA resistance to different β-lactam antibiotics [38]. PBP2a (PDB ID, 3ZFZ) used in the modeling studies has been crystallized with the inhibitor ceftaroline [37]. The celastroloids, balaenol (**12**) and zeylasterone (**14**) were found to bind to different sides of the protein active site, but both inhibitors interact with important residues of PBP2a (Figure 2I). Balaenol (**12**) showed four favorable hydrogen bonds and three hydrophobic interactions with the active site residues, including Lys406, Tyr446, Asn464, Gln 521, and Glu602 residues (Figure 2G and 2I, Table S6). Zeylasterone (**14**) showed five hydrogen bonds to Ser462, His583, Ser598, and Thr600 residues, and a favorable electrostatic interaction with the Lys597 residue (Figures 2H and 2I, Table S6).

Secreted aspartic proteinase (SAP2 - candidapepsin 2) is a virulence factor related to the biofilm-forming in *Candida* species and it is considered a new antifungal target for drug discovery [39,40]. SAP2 (PDB ID, 1EAG) used herein for modeling has been crystallized with the inhibitor A70450 (a synthetic hexapeptide analogue) [41]. Zeylasteral (**15**) showed three favorable hydrogen

bonds and five hydrophobic interactions with conserved residues within SAP2 binding site including Asp32, Asp86, Asp218, and with Val12 (Figures 3A–B, Table S7).

N-myristoyltransferase (Nmt) is an enzyme responsible for catalyzing the transfer of the fatty acid myristate from myristoyl-CoA to the N-terminal glycine residue in several eukaryotic and viral proteins and it participates in different biological processes such as signal transduction cascades and apoptosis [42]. Nmt is an essential enzyme for *C. albicans* viability and an attractive target for antimicrobial drug discovery [43,44]. Nmt used for modeling (PDB ID, 1IYL) has been crystallized with the peptidomimetic inhibitor SC-58272 [42]. Zeylasteral (**15**) showed one hydrogen bond, six hydrophobic interactions, and underwent π-stacking interactions with different residues in the active site, including the Tyr225 and Tyr354 residues, which are crucial for the protein pocket architecture [42] (Figures 3C–D, Table S8).

Bromodomain-containing factor 1 (Bdf1) is a transcription factor from the bromo- and extra-terminal domain (BET) family that regulates transcription and chromatin remodeling [45,46]. Although BD proteins are found in several eukaryotic cells, Bdf1 was identified as an antifungal drug target responsible for viability and virulence in *Candida* species [46]. Bdf1 used for modeling (PDB ID, 5N16) has been crystallized with an inhibitor derived from dibenzothiazepinone [46]. Zeylasteral (**15**) showed four favorable hydrogen bonds and four hydrophobic interactions with Val232, Pro233, Leu235, His236 Val238, Asp239, and Leu243 residues (Figure 3E-F, Table S9).

Our results indicated that some celastroloids and their derivatives can act on multi-targets by different molecular mechanisms for bacteria and fungi. However, based on the docking scores obtained we can suggest that balaenol (**12**) and zeylasterone (**14**) would inhibit GyrB rather than DHFR and PBP2a in *S. aureus* (Supplementary data, Table S4-S6), and zeylasteral (**15**) would inhibit Bdf1 rather than SAP2 and Nmt in *C. albicans* (Supplementary data, Table S7-S9).

Conclusion

Among celastroloids and their derivatives tested, most QMTs had antibacterial activity against *S. aureus* and all 14(15)-eneQMTs showed antifungal activity against *C. albicans*. The combined

analyses of the antimicrobial and cytotoxic activities of celastroloids suggested that balaenol (**12**) and zeylasterone (**14**) are promising lead candidates against *S. aureus*, whereas zeylasteral (**15**) is an attractive antifungal lead candidate with pronounced activity against *C. albicans*. The molecular docking results suggest that the most potent celastroloids could act on different targets in *S. aureus* and *C. albicans*. Although further studies are necessary to understand the exact mechanism of action, the results obtained herein provide valuable information for the future development of naturally-occurring celastroloids as antimicrobial drug candidates.

Experimental

Celastroloids and their Derivatives

The celastroloids and their derivatives (Figure 1) were obtained from our compound library which have been previously characterized using a variety of spectroscopic techniques: tingenone (**1**) [9], tingenol (**2**) [9], celastrol (**3**) [47], pristimerin (**4**) [12], 30-hydroxypristimerin (**5**) [48], 22β-hydroxytingenone (**6**) [10], 20α-hydroxytingenone (**7**) [10], isoiguesterin (**8**) [49], isoiguesterinol (**9**) [48], balaenonol (**10**) [10], isobalaendiol (**11**) [10], balaenol (**12**) [10], isobalaenol (**13**) [10], zeylasterone (**14**) [49], zeylasteral (**15**) [11], trimethylzeylasterone (**16**) [50], pristimerinene (**17**) [10], dimethylpristimerol (**18**) [12], and pristimerin diacetate (**19**) [11].

Since some celastroloids were found to undergo decomposition under HPLC conditions, all compounds were purified by repeated TLC on silica gel 60 F254 (Merck, Darmstadt, Germany); visualization under UV and by using a solution of anisaldehyde in H_2SO_4 followed by heating. All compounds used in this study were shown to be >95% pure by high-resolution ^{1}H NMR analysis. To determine the structure-activity relationships, celastroloids were separated in three groups: A) quinonemethide triterpenes (QMTs); B) 14(15)-enequinonemethide triterpenes; and C) derivatives of pristimerin which include the phenolic triterpenoids.

Antimicrobial assays

The celastroloids and their derivatives (**1–19**, Figure 1) were evaluated against the microorganisms *Escherichia coli* ATCC 25922, *Pseudomonas aeruginosa* ATCC 10197, *Staphylococcus aureus*

ATCC 25923, *S. aureus* MRSA ATCC 33592, *S. aureus* STA6 (clinical isolate), and *Candida albicans* ATCC 10261. *E. coli* ATCC 25922, *P. aeruginosa* ATCC 10197, *S. aureus* ATCC 25923, and *C. albicans* ATCC 10261 were purchased from ATCC (American Type Culture Collection). *S. aureus* MRSA ATCC 33592 was kindly provided by Dr. Michael D. L. Johnson from the College of Medicine, Department of Immunobiology, The University of Arizona, Tucson, USA. *S. aureus* STA6 (clinical isolate) was kindly provided by Dr. István Molnár, from the Southwest Center for Natural Products Research, College of Agriculture and Life Sciences, The University of Arizona, Tucson, USA.

The minimum inhibitory concentration (MIC) (CLSI M7-A9 [51], bacteria, and M27-A2 [52], yeast) and the minimum bactericidal/fungicidal concentration [53] (MBC/MFC) were performed by the micro-dilution method in 96-well plates. Broth Mueller Hinton (MH) and RPMI-1640 plus L-glutamine and MOPS acid [3-(N-morpholino)propanesulfonic acid, 0.165 mol/L] were used for bacteria and yeast, respectively.

For antibacterial assay, bacterial cultures grown for 24 h at 37 °C in MH agar were adjusted in saline solution (0.85%) by the spectrophotometer (OD550, 0.1-0.125 of absorbance) to a concentration of 1-2 x 10^8 CFU/mL. Inoculums were prepared in MH broth to a concentration of approximately 4 x 10^5 CFU/mL and diluted again in the wells containing the compounds and media to a final concentration of approximately 2 x 10^5 CFU/mL. The yeast culture grown for 24 h at 37 °C in MH agar was adjusted in saline solution by the spectrophotometer (OD530, 74-76% of transmittance) to a concentration of 1–5 x 10^6 CFU/mL and diluted in RPMI to a concentration of approximately 1 x 10^3 CFU/mL. After the addition of the yeast solution in the wells containing the compounds and RPMI, the final concentration was approximately 0.5 x 10^3 CFU/mL. All plates were maintained at 37 °C for 24 h and the MIC value was the lowest concentration of antimicrobial agent that completely inhibited visible growth. MBC/MFC assays were conducted by using 100 μL of MH or RPMI and 10 μL of the material obtained in the MIC assays. The plates were maintained under the same conditions as described above and the lowest concentration of no visible growth was considered the MBC/MFC. All assays were performed in triplicate.

Concentrations of compounds (**2–4**, **7–19**) used ranged between 100 and 0.39 µg/mL in the preliminary experiments used in this study. The concentration of compounds **1**, **5**, and **6** ranged between 100 and 0.049 µg/mL. The compounds (200 µg/mL) were solubilized in culture medium and DMSO (maximum 4%). For MRSA and STA6 the concentration ranged between 50 and 0.19 µg/mL. Positive and negative microbial growth controls were also included. In all antimicrobial studies a negative control containing the same concentration of DMSO was used. Gentamicin and amphotericin B were used as positive control for bacteria and yeast, respectively, at concentrations ranging from 50 to 0.19 µg/mL. Vancomycin was used as positive control for MRSA.

Cytotoxic assay

The human normal foreskin fibroblast (WI-38) cells were obtained from the National Cancer Institute (NCI, USA). The MTT assay was used for evaluating cytotoxicity of compounds **1–6**, **12**, **14**, and **15**. Doxorubicin and DMSO were used as positive and negative controls, respectively. The assay was performed in Eagle`s Minimum Essential Medium with 10% of FBS. Briefly, 5000 cells/well were incubated overnight at 37 °C in 96-well microtiter plates. Serial dilutions of compounds in DMSO or the vehicle control (DMSO) were added to quadruplicate wells, and the microtiter plates were incubated for a further 72 h. Viable cell number was determined by the addition of MTT, plates were incubated for 3.5–4.0 h, and then the absorbance (A) was measured at 570 nm. Cytotoxicity was calculated using the following formula: % cytotoxicity = $[(A_{Medium} - A_{Treatment})/A_{Medium}] \times 100$. The IC_{50} values and standard deviations (±) were determined using Microsoft Excel software from dose-response curves obtained from at least three independent experiments.

Docking studies

An *in-silico* screening with different *S. aureus* and *C. albicans* essential and potential proteins were performed in order to predict the theoretical affinity binding of the most active triterpenes and to estimate their possible mechanism of action.

Ligand preparation: The ligands structures were sketched in 2D using BKChem 0.13.0 [54] and converted to 3D models with Open Babel 3.0.1 [55] using the *--gen3d best* option. Hydrogens appropriate for pH 7.4 were added using Avogadro 1.2.0 [56] and then these structures were optimized using the semi-empirical method PM7 [57] available in MOPAC2016 [58]. UCSF Chimera 1.14 [59] was used to add Gasteiger charges [60] to the ligands and, finally, the active torsions of all molecules were manually defined using the AutoDockTools 1.5.6 software [61].

Protein preparation: All 3D structures were downloaded from the Protein Data Bank (PDB; https://www.rcsb.org). The molecular targets investigated herein included are, *S. aureus*: DNA gyrase subunit B (topoisomerase - gyrB) – PDB code 3TTZ, Dihydrofolate reductase (DHFR) – PDB code 3FYW, and Penicillin binding protein 2a (PBP2a) – PDB code 3ZFZ; *C. albicans*: the proteins were Secreted aspartic proteinase (candidapepsin 2) – PDB code 1EAG, Glyculpeptide N-tetradecanoyltransferase (N-myristoyltransferase - Nmt) – PDB code 1IYL, and Bromodomain-containing factor 1 (BDF1) – PDB code 5N16. For docking, incomplete side chains of structures were automatically reconstructed using Swiss-pdb Viewer 4.1.0 [62]. All solvents, ligands and cofactors were removed and polar H atoms were added by Gasteiger charges calculation using AutoDock Tools 1.5.6 [63].

Molecular docking: All molecular docking calculations were carried out using Autodock Vina 1.1.2 [64]. The values of X, Y, and Z axis (docking area) were taken from the substrate-binding pockets and according to the size of each ligand. The docked complexes were ranked according to their energy scores and their molecular interactions were analyzed using Protein-Ligand Interaction Profiler (PLIP) [65]. The graphical depictions of ligand-protein complexes were plotted by UCSF Chimera and PyMOL 2.3 [66]. Re-docking experiments with the co-crystallized ligands were carried out to validate the docking protocol being used.

Acknowledgments We thank Sao Paulo Research Foundation – FAPESP for funding (2013/07600-3 and 2020/12904-5 to R. V. C. Guido) and research fellowships (2014/19362-2 and 2018/00143-0 to M. C. Inacio). We also thank Dr. Michael D. L. Johnson from the College of

Medicine, Department of Immunobiology, The University of Arizona, Tucson, USA for kindly providing the MRSA strain and Dr. István Molnár from the Southwest Center for Natural Products Research, College of Agriculture and Life Sciences, The University of Arizona, Tucson, USA for kindly providing the STA6 strain.

Compliance with ethical standards

Conflict of interest The authors declare that they have no known competing financial interests or personal relationships that could have appeared to influence the work reported in this paper.

Publisher's note Springer Nature remains neutral with regard to jurisdictional claims in published maps and institutional affiliations.

Supplementary information The online version contains supplementary material available at https://doi.org/10.1007/s00044-xxx-xxxxx-x.

References

1. WHO. WHO | Prioritization of Pathogens to Guide Discovery, Research and Development of New Antibiotics for Drug Resistant Bacterial Infections, Including Tuberculosis. Geneva: World Health Organization; 2017.
2. Khameneh B, Iranshahy M, Soheili V, Fazly Bazzaz BS. Review on plant antimicrobials: a mechanistic viewpoint. Antimicrob Resist Infect Control. 2019;8(1):1-28. https://doi:10.1186/s13756-019-0559-6.
3. Igarashi M. New natural products to meet the antibiotic crisis: a personal journey. J Antibiot. 2019;72(12):890-898. https://doi:10.1038/s41429-019-0224-6.
4. Li G, Lou H-X. Strategies to diversify natural products for drug discovery. Med Res Rev. 2018;38(4):1255-1294. https://doi:10.1002/med.21474.
5. Catteau L, Zhu L, Van Bambeke F, Quetin-Leclercq J. Natural and hemi-synthetic pentacyclic triterpenes as antimicrobials and resistance modifying agents against *Staphylococcus aureus*: a review. Phytochem Rev. 2018;17(5):1129-1163. https://doi:10.1007/s11101-018-9564-2.

6. Jesus JA, Lago JHG, Laurenti MD, Yamamoto ES, Passero LFD. Antimicrobial activity of oleanolic and ursolic acids: an update. Evid Based Complement Alternat Med. 2015;2015:620472. https://doi:10.1155/2015/620472.
7. De León L, Beltrán B, Moujir L. Antimicrobial activity of 6-oxophenolic triterpenoids. Mode of action against *Bacillus subtilis*. Planta Med. 2005;71(4):313-319. https://doi:10.1055/s-2005-864096.
8. Gullo FP, Sardi JCO, Santos VAFFM, et al. Antifungal activity of maytenin and pristimerin. Evidence-Based Complement. Altern. Med. 2012;2012: 340787. https://doi:10.1155/2012/340787.
9. Inácio MC, Paz TA, Pereira AMS, Furlan M. Endophytic *Bacillus megaterium* and exogenous stimuli affect the quinonemethide triterpenes production in adventitious roots of *Peritassa campestris* (Celastraceae). Plant Cell, Tissue Organ Cult. 2017;131(1):15-26. https://doi:10.1007/s11240-017-1257-9.
10. Fernando HC, Gunatilaka AAL, Tezuka Y, Kikuchi T. Studies on terpenoids and steroids - 18 balaenonol, balaenol and isobalaendiol: three new 14(15)-ene-quinone-methide triterpenoids from *Cassine balae*. Tetrahedron. 1989;45(18):5867-5876. https://doi:10.1016/S0040-4020(01)89113-4.
11. Gamlath CB, Gunaherath GMKB, Gunatilaka AAL. Studies on terpenoids and steroids. Part 10. Structures of four new natural phenolic D:A-*friedo*-24-noroleanane triterpenoids. J Chem Soc Perkin Trans 1. 1987:2849-2854. https://doi:10.1039/P19870002849.
12. Gunaherath GMKB, Gunatilaka AAL. Studies on terpenoids and steroids. Part 3. Structure and synthesis of a new phenolic D:A-*friedo*-24-noroleanane triterpenoid, zeylasterone, from *Kokoona zeylanica*. J Chem Soc Perkin Trans 1. 1983:2845-2850. https://doi:10.1039/P19830002845.
13. Tezuka Y, Kikuchi T, Dhanabalasingham B, Karunaratne V, Gunatilaka AAL. Studies on terpenoids and steroids, 25. Complete 1H- and 13C-nmr spectral assignments of

salaciquinone, a new 7-oxo-quinonemethide dinortriterpenoid. J Nat Prod. 1994;57(2):270-276. https://doi:10.1021/np50104a012.

14. González AG, Bazzocchi IL, Moujir L, Jiménez IA. Ethnobotanical uses of celastraceae. Bioactive metabolites. Studies in Natural Products Chemistry. 2000;23:649-738. https://doi:10.1016/S1572-5995(00)80140-4.
15. De Souza GC, Haas APS, von Poser GL, Schapoval EES, Elisabetsky E. Ethnopharmacological studies of antimicrobial remedies in the south of Brazil. J Ethnopharmacol. 2004;90(1):135-143. https://doi:10.1016/j.jep.2003.09.039.
16. Gunatilaka AAL. Triterpenoid Quinonemethides and Related Compounds (Celastroloids). In: Herz W, Kirby GW, Moore RE Steglich W, Tamm C, editors. Fortschritte Der Chemie Organischer Naturstoffe/Progress in the Chemistry of Organic Natural Products. Vol 67. Vienna: Springer Vienna; 1996. p.1-123.
17. De León L, Moujir L. Activity and mechanism of the action of zeylasterone against *Bacillus subtilis*. J Appl Microbiol. 2008;104(5):1266-1274. https://doi:10.1111/j.1365-2672.2007.03663.x.
18. González AG, Alvarenga NL, Ravelo AG, et al. Antibiotic phenol nor-triterpenes from *Maytenus canariensis*. Phytochemistry. 1996;43(1):129-132. https://doi:10.1016/0031-9422(96)00205-1.
19. Sotanaphun U, Lipipun V, Suttisri R, Bavovada R. Antimicrobial activity and stability of tingenone derivatives. Planta Med. 1999;65(05):450-452. https://doi:10.1055/s-2006-960809.
20. Moujir L, Gutierrez-Navarro AM, Gonzalez AG, Ravelo AG, Luis JG. Mode of action of netzahualcoyone. Antimicrob Agents Chemother. 1991;35(1):211-213. https://doi:10.1128/AAC.35.1.211.
21. Rodríguez FM, López MR, Jiménez IA, Moujir L, Ravelo AG, Bazzocchi IL. New phenolic triterpenes from *Maytenus blepharodes*. Semisynthesis of 6-deoxoblepharodol from pristimerin. Tetrahedron. 2005;61(9):2513-2519. https://doi:10.1016/j.tet.2004.12.046.

22. González AG, Alvarenga NL, Ravelo AG, et al. Scutione, a new bioactive norquinonemethide triterpene from *Maytenus scutioides* (Celastraceae). Bioorganic Med Chem. 1996;4(6):815-820. https://doi:10.1016/0968-0896(96)00078-8.

23. Moujir L, R. López M, P. Reyes C, Jiménez IA, L. Bazzocchi I. Structural requirements for antimicrobial activity of phenolic nor-triterpenes from Celastraceae species. *Appl Sci*. 2019;9(15):2957. https://doi:10.3390/app9152957.

24. Moujir L, Gutiérrez-Navarro AM, González AG, Ravelo AG, Luis JG. The relationship between structure and antimicrobial activity in quinones from the Celastraceae. Biochem Syst Ecol. 1990;18(1):25-28. https://doi:10.1016/0305-1978(90)90028-E.

25. Saleem M, Nazir M, Ali MS, et al. Antimicrobial natural products: an update on future antibiotic drug candidates. Nat Prod Rep. 2010;27(2):238-254. https://doi:10.1039/b916096e.

26. Hu X-L, He Q-W, Long H, et al. Synthesis and biological evaluation of celastrol derivatives with improved cytotoxic selectivity and antitumor activities. J Nat Prod. 2021;84(7):1954-1966. https://doi:10.1021/ACS.JNATPROD.1C00262.

27. Lu Y, Liu Y, Zhou J, Li D, Gao W. Biosynthesis, total synthesis, structural modifications, bioactivity, and mechanism of action of the quinone-methide triterpenoid celastrol. Med Res Rev. 2021;41(2):1022-1060. https://doi:10.1002/MED.21751.

28. de León L, López MR, Moujir L. Antibacterial properties of zeylasterone, a triterpenoid isolated from *Maytenus blepharodes*, against *Staphylococcus aureus*. Microbiol Res. 2010;165(8):617-626. https://doi:10.1016/j.micres.2009.12.004.

29. López MR, De León L, Moujir L. Antibacterial properties of phenolic triterpenoids against *Staphylococcus epidermidis*. *Planta Med*. 2011;77(7):726-729. https://doi:10.1055/s-0030-1250500.

30. dos Santos RN, Ferreira LG, Andricopulo AD. Practices in molecular docking and structure-based virtual screening. In: Gore M., Jagtap U., eds. Computational Drug Discovery and Design. Methods in Molecular Biology. Vol 1762. New York: Humana Press Inc.; 2018. p.31-50.

31. Barman TK, Kumar M, Mathur T, et al. In vitro and in vivo activities of DS-2969b, a novel GyrB inhibitor, and its water-soluble prodrug, DS11960558, against methicillin-resistant *Staphylococcus aureus*. Antimicrob Agents Chemother. 2018;62(6): e02556-17. https://doi:10.1128/AAC.02556-17.
32. Durdagi S, Tahir ul Qamar M, Salmas RE, Tariq Q, Anwar F, Ashfaq UA. Investigating the molecular mechanism of staphylococcal DNA gyrase inhibitors: A combined ligand-based and structure-based resources pipeline. J Mol Graph Model. 2018;85:122-129. https://doi:10.1016/J.JMGM.2018.07.010.
33. Sherer B, Hull K, Green O, et al. Pyrrolamide DNA gyrase inhibitors: optimization of antibacterial activity and efficacy. Bioorg Med Chem Lett. 2011;21(24):7416-7420. https://doi:10.1016/J.BMCL.2011.10.010.
34. Reeve SM, Si D, Krucinska J, et al. Toward broad spectrum dihydrofolate reductase inhibitors targeting trimethoprim resistant enzymes identified in clinical isolates of methicillin resistant *Staphylococcus aureus*. ACS Infect Dis. 2019;5(11):1896-1906. https://doi:10.1021/ACSINFECDIS.9B00222.
35. Lade H, Kim J-S. Bacterial targets of antibiotics in Methicillin-Resistant *Staphylococcus aureus*. Antibiot. 2021;10(4):398. https://doi:10.3390/ANTIBIOTICS10040398.
36. Oefner C, Parisi S, Schulz H, Lociuro S, Dale GE How allosteric control of *Staphylococcus aureus* penicillin binding protein. Inhibitory properties and X-ray crystallographic study of the binding of AR-101, AR-102 and iclaprim in ternary complexes with NADPH and dihydrofolate reductase from *Staphylococcus aureus*. Acta Crystallogr D Biol Crystallogr. 2009;65(Pt 8):751-757. https://doi:10.1107/S0907444909013936.
37. Otero LH, Rojas-Altuve A, Llarrull LI, et al. How allosteric control of *Staphylococcus aureus* penicillin binding protein 2a enables methicillin resistance and physiological function. Proc Natl Acad Sci USA. 2013;110(42):16808-16813. https://doi:10.1073/PNAS.1300118110.

38. Shalaby MAW, Dokla EME, Serya RAT, Abouzid KAM. Penicillin binding protein 2a: an overview and a medicinal chemistry perspective. Eur J Med Chem. 2020;199:112312. https://doi:10.1016/J.EJMECH.2020.112312.

39. Li C, Liu Y, Wu S, Han G, Tu J, Dong G, Liu N, Sheng C. Targeting fungal virulence factor by small molecules: structure-based discovery of novel secreted aspartic protease 2 (SAP2) inhibitors. Eur J Med Chem. 2020;201:112515. https://doi:10.1016/J.EJMECH.2020.112515.

40. Meenambiga SS, Venkataraghavan R, Biswal RA. *In silico* analysis of plant phytochemicals against secreted aspartic proteinase enzyme of *Candida albicans*. J Appl Pharm Sci. 2018;8(11):140-150. https://doi:10.7324/JAPS.2018.81120.

41. Cutfield S, Dodson E, Anderson B, et al. The crystal structure of a major secreted aspartic proteinase from *Candida albicans* in complexes with two inhibitors. Structure. 1995;3(11):1261-1271. https://doi:10.1016/S0969-2126(01)00261-1.

42. Sogabe S, Masubuchi M, Sakata K, et al. Crystal structures of *Candida albicans* N-myristoyltransferase with two distinct inhibitors. Chem Biol. 2002;9(10):1119-1128. https://doi:10.1016/S1074-5521(02)00240-5.

43. Dabade SJ, Mandloi D, Bajaj A V., Thakur A. In silico evaluation of inhibitory potential of novel triazole derivatives against therapeutic target myristoyl-CoA: protein N-myristoyltransferase (NMT) of *Candida albicans*. Netw Model Anal Heal Informatics Bioinform. 2020;9:60. https://doi:10.1007/S13721-020-00265-4.

44. Garcia ML, de Oliveira AA, Bueno RV., et al. QSAR studies on benzothiophene derivatives as *Plasmodium falciparum* N-myristoyltransferase inhibitors: molecular insights into affinity and selectivity. Drug Dev Res. 2020. https://doi:10.1002/DDR.21646.

45. Winston F, Allis CD. The bromodomain: a chromatin-targeting module? Nat Struct Biol. 1999;6(7):601-604. https://doi:10.1038/10640.

46. Mietton F, Ferri E, Champleboux M, et al. Selective BET bromodomain inhibition as an antifungal therapeutic strategy. Nat Commun. 2017;8(1): 15482. https://doi:10.1038/ncomms15482.

47. Gamlath CB, Gunatilaka AAL, Tezuka Y, Kikuchi T, Balasubramaniam S. Quinone-methide, phenolic and related triterpenoids of plants of Celastraceae: further evidence for the structure of Celastranhydride. Phytochemistry. 1990;29(10):3189-3192. https://doi:10.1016/0031-9422(90)80182-G.

48. Dhanabalasingham B, Karunaratne V, Tezuka Y, Kikuchi T, Gunatilaka AAL. Biogenetically important quinonemethides and other triterpenoid constituents of *Salacia reticulata*. Phytochemistry. 1996;42(5):1377-1385. https://doi:10.1016/0031-9422(96)00886-2.

49. Sneden AT. Isoiguesterin, a new antileukemic bisnortriterpene from *Salacia madagascariensis*. J Nat Prod. 1981;44(4):503-507. https://doi:10.1021/NP50016A023.

50. Gunaherath GMKB, Gunatilaka AAL, Sultanbawa MUS, Wazeer MIM. The structure of zeylasterone - the first of a new series of phenolic 24-nor-D:A-friedo-oleanan triterpenes. Tetrahedron Lett. 1980;21(49):4749-4752. https://doi:10.1016/0040-4039(80)88112-3.

51. CLSI. Methods for Dilution Antimicrobial Susceptibility Tests for Bacteria That Grow Aerobically; Approved Standard-9th Edition. CLSI document M07-A9: Wayne, PA: Clinical and Laboratory Standards Institute; 2012.

52. CLSI. Reference Method for Broth Dilution Antifungal Susceptibility Testing of Yeasts; Apprved standard 2nd Edition. NCCLS document M27-A2: Wayne, PA: National Committee for Clinical Laboratory Standards; 2002.

53. Hernandes C, Coppede J da S, Bertoni BW, França S de C, Pereira AMS. Flash microbiocide: a rapid and economic method for determination of MBC and MFC. Am J Plant Sci. 2013;4:850-852. https://doi:10.4236/ajps.2013.44104.

54. Pirhadi S, Sunseri J, Koes DR. Open source molecular modeling. J Mol Graph Model. 2016;69:127-143. https://doi:10.1016/j.jmgm.2016.07.008.

55. O'Boyle NM, Banck M, James CA, Morley C, Vandermeersch T, Hutchison GR. Open Babel: an open chemical toolbox. J Cheminform. 2011;3:33. doi:10.1186/1758-2946-3-33.

56. Hanwell MD, Curtis DE, Lonie DC, Vandermeersch T, Zurek E, Hutchison GR. Avogadro: an advanced semantic chemical editor, visualization, and analysis platform. J Cheminform. 2012;4:17. https://doi:10.1186/1758-2946-4-17.

57. Stewart JJP. Application of localized molecular orbitals to the solution of semiempirical self-consistent field equations. Int J Quantum Chem. 1996;58(2):133-146. https://doi:10.1002/(SICI)1097-461X(1996)58:2<133::AID-QUA2>3.0.CO;2-Z.

58. Stewart JJP. Stewart Computational Chemistry - MOPAC Home Page. http://openmopac.net/. Published 2016. Accessed August 26, 2021.

59. Pettersen EF, Goddard TD, Huang CC, et al. UCSF Chimera - A visualization system for exploratory research and analysis. J Comput Chem. 2004;25(13):1605-1612. https://doi:10.1002/jcc.20084.

60. Wang J, Wang W, Kollman PA, Case DA. Automatic atom type and bond type perception in molecular mechanical calculations. J Mol Graph Model. 2006;25(2):247-260. https://doi:10.1016/J.JMGM.2005.12.005.

61. Goodsell DS, Morris GM, Olson AJ. Automated docking of flexible ligands: applications of autodock. J Mol Recognit. 1996;9(1):1-5. https://doi:10.1002/(SICI)1099-1352(199601)9:1%3C1::AID-JMR241%3E3.0.CO;2-6.

62. Guex N, Peitsch MC. SWISS-MODEL and the Swiss-PdbViewer: an environment for comparative protein modeling. Electrophoresis. 1997;18(15):2714-2723. https://doi:10.1002/elps.1150181505.

63. Goodsell DS, Olson AJ. Automated docking of substrates to proteins by simulated annealing. Proteins Struct Funct Bioinforma. 1990;8(3):195-202. https://doi:10.1002/PROT.340080302.

64. Trott O, Olson AJ. AutoDock Vina: improving the speed and accuracy of docking with a new scoring function, efficient optimization, and multithreading. J Comput Chem. 2010;31(2): 455-461. https://doi:10.1002/jcc.21334.

65. Adasme MF, Linnemann KL, Bolz SN, et al. PLIP 2021: expanding the scope of the protein–ligand interaction profiler to DNA and RNA. Nucleic Acids Res. 2021;49(W1):W530-W534. https://doi:10.1093/NAR/GKAB294.

66. DeLano WL. PyMOL: An Open-Source Molecular Graphics Tool. *CCP4 Newsl Protein Crystallogr*. 2002;40(1):44-53. http://legacy.ccp4.ac.uk/newsletters/newsletter40.pdf.

Table 1
Minimum inhibitory concentration (MIC) and minimum bactericide/fungicide concentration (MBC/MFC) of the quinonemethides triterpenes (**1–9**) against the microorganisms *Staphylococcus aureus* ATCC 25923, *S. aureus* MRSA ATCC 33592, *S. aureus* STA6 clinical isolate, and *Candida albicans* ATCC 10261. Results are expressed in μg/mL.

Compound	Functional groups in ring E	*S. aureus* ATCC 25923		*S. aureus* MRSA ATCC 33592		*S. aureus* STA6		*C. albicans* ATCC 10261	
		MIC	MBC	MIC	MBC	MIC	MBC	MIC	MFC
Tingenone (1)	C-21 =O	0.39	1.56	0.39	6.25	1.56	6.25	50	>100
Tingenol (2)	C-21 β-OH	0.78	6.25	0.78	6.25	3.12	25	50	>100
Celastrol (3)	C-20 α-CO_2H	0.78	12.5	0.39	6.25	0.78	12.5	6.25	100
Pristimerin (4)	C-20 α-CO_2Me	12.5	100	1.56	25	12.5	50	25	>100
30-Hydroxypristimerin (5)	C-20 α-CO_2Me; C-20 β-CH_2OH	0.39	0.78	0.39	6.25	1.56	25	6.25	50
22β-Hydroxytingenone (6)	C-21 =O; C-22 β-OH	0.39	3.13	0.78	6.25	1.56	6.25	50	>100
20α-Hydroxytingenone (7)	C-21 =O; C-20 α-OH	0.78	6.25	1.56	6.25	1.56	12.5	50	>100
Isoiguesterin (8)	C-20 =CH_2	100	>100	6.25	25	50	>50	>100	NT
Isoiguesterinol (9)	C-30 OH	1.56	50	0.39	1.56	1.56	25	>100	NT

NT = not tested

Table 2
Minimum inhibitory concentration (MIC) and minimum bactericide/fungicide concentration (MBC/MFC) of the 14(15)-enequinomethide triterpenes (**10–13**) against the microorganisms *Staphylococcus aureus* ATCC 25923, *S. aureus* MRSA ATCC 33592, *S. aureus* STA6 clinical isolate and *Candida albicans* ATCC 10261. Results are expressed in μg/mL.

Compound	Functional groups in ring E	*S. aureus* ATCC 25923		*S. aureus* MRSA ATCC 33592		*S. aureus* STA6		*C. albicans* ATCC 10261	
		MIC	MBC	MIC	MBC	MIC	MBC	MIC	MFC
Balaenonol (10)	C-21 β-OH; C-22 =O	1.56	6.25	1.56	6.25	0.78	6.25	12.5	12.5
Isobalaendiol (11)	C-21 β-OH; C-22 β-OH	6.25	50	3.12	25	6.25	50	12.5	25
Balaenol (12)	C-21 β-OH; C-20 β-Me	1.56	12.5	0.19	1.56	1.56	25	3.12	100
Isobalaenol (13)	C-21 β-OH; C-20 α-Me	1.56	12.5	3.12	25	6.25	25	6.25	6.25

Table 3
Minimum inhibitory concentration (MIC) and minimum bactericide/fungicide concentration (MBC/MFC) of pristimerin, phenolic triterpenes and their derivatives (**4, 14–19**) against the microorganisms *Staphylococcus aureus* ATCC 25923, *S. aureus* MRSA ATCC 33592, *S. aureus* STA6 clinical isolate and *Candida albicans* ATCC 10261. Results are expressed in μg/mL.

Compound	Functional groups in rings A, B and C	*S. aureus* ATCC 25923		*S. aureus* MRSA ATCC 33592		*S. aureus* STA6		*C. albicans* ATCC 10261	
		MIC	MBC	MIC	MBC	MIC	MBC	MIC	MFC
Pristimerin (4)	C-2 =O; C-3 OH	12.5	100	1.56	25	12.5	50	25	>100
Zeylasterone (14)	C-2 OH; C-3 OH; C-4 CO_2H; C-6 =O	1.56	25	1.56	12.5	1.56	6.25	6.25	6.25
Zeylasteral (15)	C-2 OH; C-3 OH; C-4 CHO; C-6 =O	50	100	25	50	12.5	50	3.12	3.12
Trimethylzeylasterone (16)	C-2 MeO; C-3 MeO; C-4 CO_2Me; C-6 =O	>100	NT	>50	NT	>50	NT	>100	NT
Pristimerinene (17)	C-2 =O; C-3 OH; C-9(11) ene	>100	NT	>50	NT	>50	NT	>100	NT
Dimethylpristimerol (18)	C-2 MeO; C-3 MeO	>100	NT	>50	NT	>50	NT	>100	NT
Pristimerin diacetate (19)	C-2 AcO; C-3 AcO	>100	NT	>50	NT	>50	NT	>100	NT

NT = not tested

Table 4
IC_{50} data (in μM and μg/mL) for antimicrobial celastroloids, tingenone (**1**), tingenol (**2**), celastrol (**3**), pristimerin (**4**), 30-hydroxypristimerin (**5**), 22β-hydroxytingenone (**6**), balaeonol (**12**), zeylasterone (**14**), and zeylasteral (**15**) against the normal human foreskin fibroblast (WI-38) cells.

Compound	WI-38	
	μM	μg/mL
Tingenone (**1**)	0.40 ± 0.09	0.17
Tingenol (**2**)	0.71 ± 0.03	0.30
Celastrol (**3**)	0.60 ± 0.07	0.27
Pristimerin (**4**)	0.35 ± 0.02	0.16
30-Hydroxypristimerin (**5**)	0.8 ± 0.1	0.36
22β-Hydroxytingenone (**6**)	0.7 ± 0.1	0.32
Balaenol (**12**)	2.9 ± 0.3	1.27
Zeylasterone (**14**)	5.6 ± 0.2	2.85
Zeylasteral (**15**)	12.9 ± 0.5	6.38

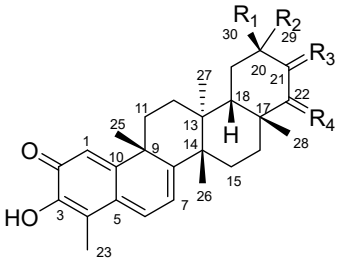

1 R_1 = Me; R_2 = H; R_3 = O; R_4 = H_2
2 R_1 = Me; R_2 = H; R_3 = β–OH,α–H; R_4 = H_2
3 R_1 = Me; R_2 = CO_2H; R_3 = R_4 = H_2
4 R_1 = M ; R_2 = CO_2Me; R_3 = R_4 = H_2
5 R_1 = CH_2OH; R_2 = CO_2Me; R_3 = R_4 = H_2
6 R_1 = Me; R_2 = H; R_3 = O; R_4 = β–OH,α–H
7 R_1 = M ; R_2 = OH; R_3 = O; R_4 = H_2
8 R_1, R_2 = CH_2; R_3 = R_4 = H_2
9 R_1 = CH_2OH; R_2 = H; R_3 = R_4 = H_2

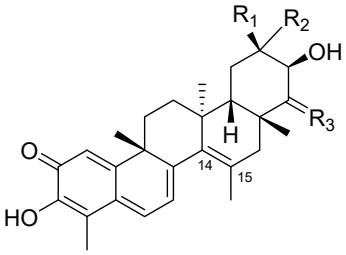

10 R_1 = Me; R_2 = H; R_3 = O
11 R_1 = H; R_2 = Me; R_3 = β–OH,α–H
12 R_1 = Me; R_2 = H; R_3 = H_2
13 R_1 = H; R_2 = Me; R_3 = H_2

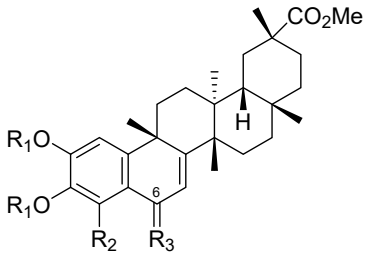

14 R_1 = H; R_2 = CO_2H; R_3 = O
15 R_1 = H; R_2 = CHO; R_3 = O
16 R_1 = Me; R_2 = CO_2Me; R_3 = O
18 R_1 = R_2 = Me; R_3 =H_2
19 R_1 = Ac; R_2 = Me; R_3 = H_2

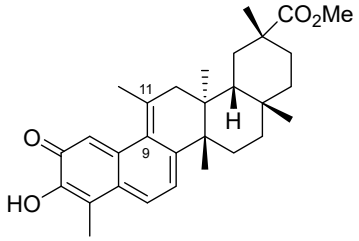

17

Figure 1. Structures of celastroloids, including quinonemethides **1**–**9** (Group A), 14(15)-enequinonemethides **10**–**13** (Group B), and derivatives of pristimerin **14**–**19** (Group C).

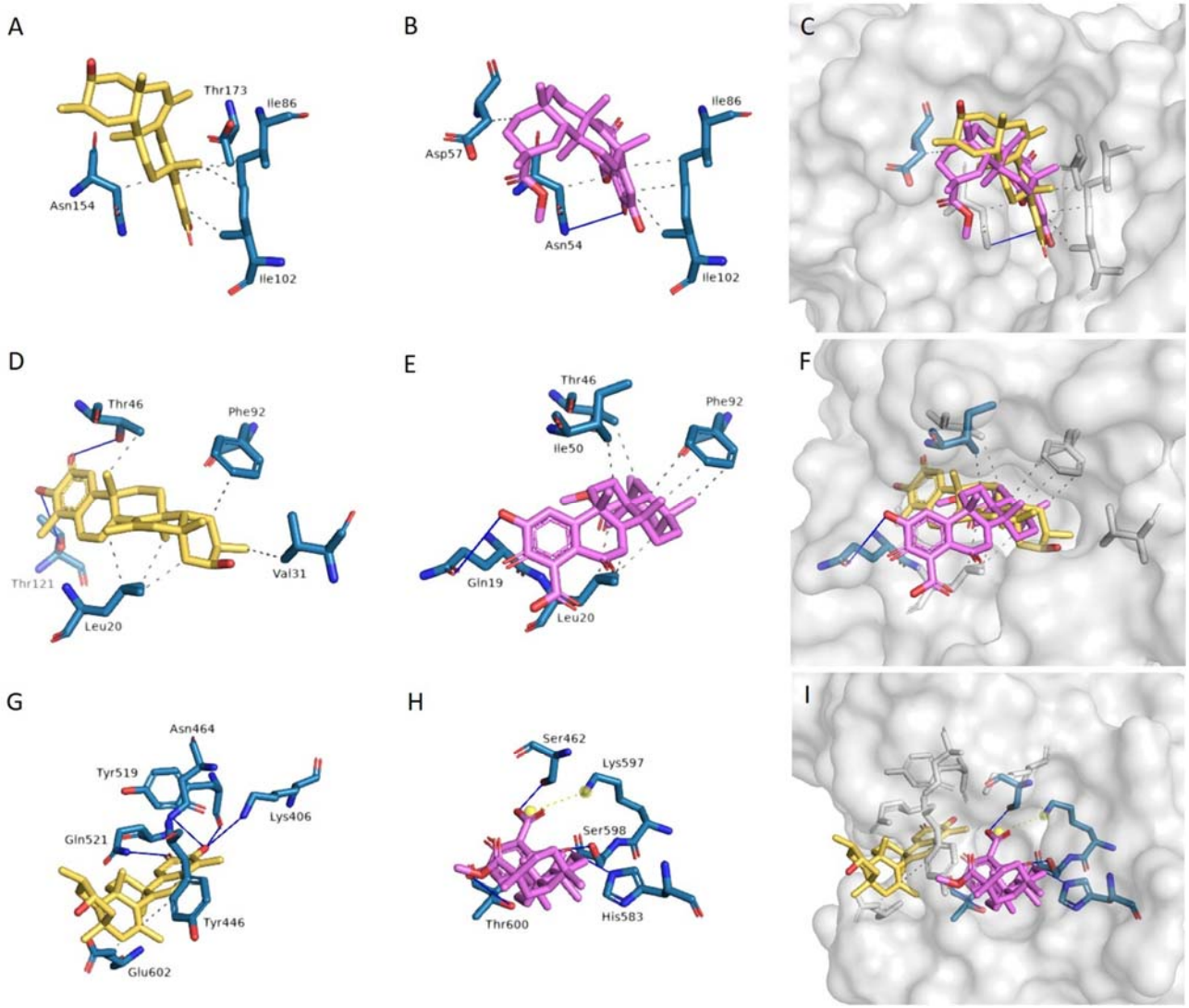

Figure 2. Binding modes of active celastroloids, balaenol (**12**, yellow) and zeylasterone (**14**, violet). **A–C**: with DNA gyrase subunit B (topoisomerase - gyrB) – PDB code 3TTZ. **D–F**: with dihydrofolate reductase (DHFR) – PDB code 3FYW: **G–I**: with Penicillin binding protein 2a (PBP2a) – PDB code 3ZFZ from *S. aureus*. For clarity, only interacting residues are labeled. Hydrogen bonding interactions are shown in blue solid lines, hydrophobic interactions in grey dashed lines, and electrostatic interactions in yellow dashed lines. Images were made using Pymol.

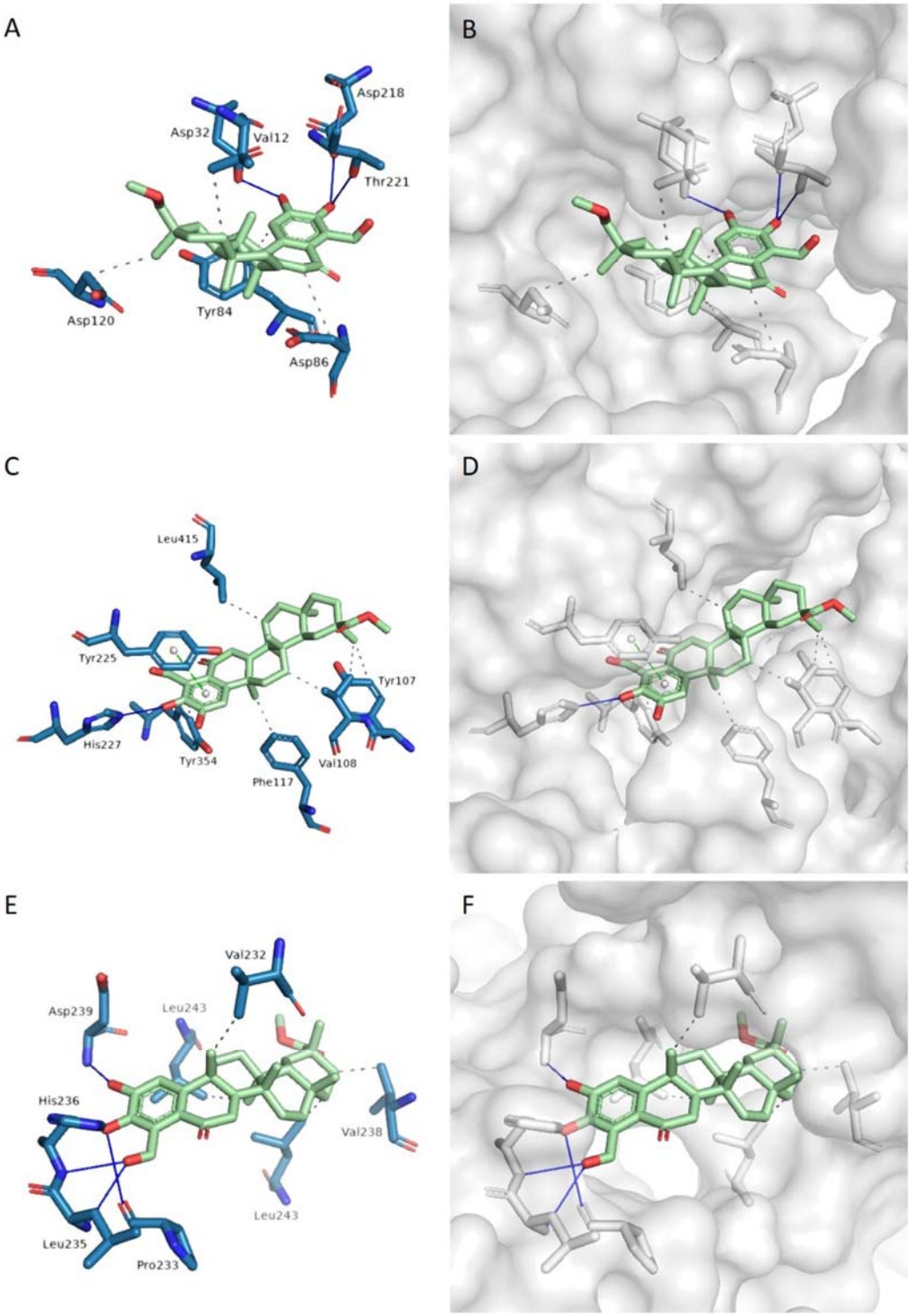

Figure 3. Binding modes of zeylasteral (**15**, green). **A–B**: with secreted aspartic proteinase (candidapepsin 2) – PDB code 1EAG. **C–D**: with *N*-myristoyltransferase (Nmt) – PDB code 1IYL. **E–F**: with bromodomain-containing factor 1 (Bdf1) – PDB code 5N16 from *C. albicans*. For clarity, only interacting residues are labeled. Hydrogen bonding interactions are shown in blue solid lines, hydrophobic interactions in grey dashed lines, and π-stacking interactions in green dashed lines. Images were made using Pymol.